Historically Consistent and Geodetically Constrained Bayesian Inference of Megathrust Rheology

Tobias Köhne[1], Rishav Mallick[1,2], Théa Ragon[1], Mark Simons[1]

[1] Seismological Laboratory, Division of Geological and Planetary Sciences, California Institute of Technology; [2] *now* NASA Jet Propulsion Laboratory

tkoehne@caltech.edu www.tobiaskoehne.de
AGU Fall Meeting 2023 T41D-0258

Timeseries Analysis: DISSTANS github.com/tobiscode/disstans
2D Forward Model: SeqEAS github.com/tobiscode/seqeas-public
Inverse Model: AlTar github.com/lijun99/altar2-documentation

I. Introduction & Motivation

- **Constraining the effective rheology of subduction zone megathrusts is crucial** to improve our understanding of the physics of convergent plate boundary deformation (e.g., Bürgmann & Dresen, 2008). Key questions include: **How does stress accumulate, release, and distribute** during the earthquake cycle? Where and how are mountain ranges sustained? How can plate-like tectonics exist? And what does our understanding imply for seismic hazard assessments?
- **Laboratory experiments** have been used to propose constitutive relations of specific rock types at the **micron to meter scale** (e.g., Blanpied et al., 1995; Hirth, 2002; Hirth & Kohlstedt, 2004).
- Postseismic displacement timeseries observations near plate interfaces have since been used to estimate ranges of parameters for such models (e.g., Freed et al., 2012; Agata et al., 2019; Muto et al., 2019; Fukuda & Johnson, 2021) although it is unclear if **geodetic evidence** can distinguish between different models at **megathrust scales**.

  → **Longterm goal:**
  Identify classes of rheological models that are internally consistent over different phases of the seismic cycle.
- We build on the concepts of Hetland & Simons (2010) and Hetland et al. (2010) that **model interseismic creep in the Northern Japan subduction zone** given a recurring rupture sequence (informed by historical seismic catalogs), locked asperity patches, and a rate-dependent frictional model.

  → **Goal for this study:**
  Develop a Bayesian framework to solve for spatially-variable rheological parameters of the Northern Japan megathrust using 3D GNSS displacement data of the entire observed post- and interseismic periods.

II. Summary

1. Build **mesh** based on plate interface geometry and **coseismic rupture extents** (center figure).
2. Define **spatially-variable profile of rate-dependent strength** parameter (Box III).
3. Based on historical catalogs, define a **rupture history** for the asperities (Box IV).
4. Solve the **initial value problem** relating external forcing (plate convergence) to frictional resistance on the plate interface, **generating model interface and surface velocities** (Box V).
5. Compare the model output with **surface observations** (Box VI).
6. Use a Markov chain Monte Carlo solver to **estimate rheological parameters** that best match surface observations (Box VII) (i.e., repeat from step 2).

III. Spatially-variable Friction

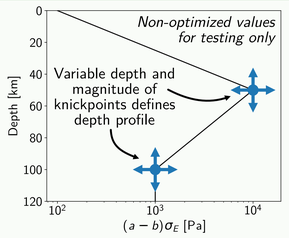

- Each patch follows **rate-dependent friction:**
  $f_{ss} = f_0 + (a\text{-}b)\ \zeta = \tau\ /\ \sigma_E$ (f_{ss} steady-state friction, f_0, a, and b constants, σ_E effective normal stress, τ shear stress, ζ logarithm of slip rate, e.g., Rice & Ruina, 1983).
- The steady-state **frictional strength (a-b) σ_E is varied** with depth based on the location of two knickpoints and logarithmic interpolation between them.
- Future work includes using splines both down-dip and along-strike to parameterize frictional strength.

Study setting. The light grey contours show Northern Japan in a slanted map view, focusing on the islands of Honshū and Hokkaidō. The subset of the continuously-operating Global Navigation Satellite System (GNSS) stations of the GEONET network used in this study are marked by grey triangles (stations 93004 is highlighted, with Box VII showing the timeseries of it). The plate interface of the Japan Trench subduction zone is shown as the depth-colored triangular mesh (based on Slab2, Hayes et al., 2018). 7 asperities with recurring earthquakes are marked with different colors and labeled with their last significant rupture and magnitude. The rupture timelines for each asperity are shown in Box IV. Asterisks mark asperities that, in our rupture timeline and forward model, also slipped during the great M_W 9.1 Tōhoku in 2011. The relative plate convergence is modeled using Euler poles for the Eurasian and Pacific plates. For the forward model in Box VI, we use a coarse version of this mesh for computational reasons. Future work will include improving the size, shape and location of the asperities.

IV. Asperity Rupture Timeline

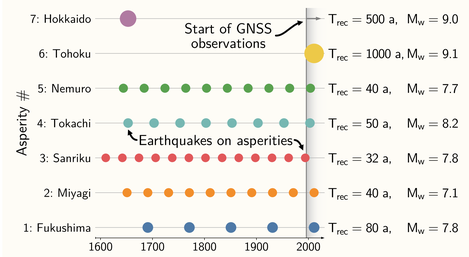

- We define an **asperity** as an area on the interface that **only slips coseismically**.
- Based on the literature and earthquake catalog review of Kanda et al. (2013), we assign a **recurrence interval and slip magnitude for each asperity**.
- Plate convergence is recovered after integration over a full cycle (e.g., 4000 a).
- Asperities are allowed to rupture jointly.

V. Forward Model

- Each **patch** is modeled as a **spring-slider system** where the resistive shear traction τ is balancing the far-field and elastic loading of the patch.
- From the **boundary integral formulation**, we get $d\tau/dt = K\ (v - v_p)$ (K stress kernel, v_p plate velocity).
- From the rheology of steady-state, **rate-dependent friction**, we get $d\tau/dt = (a\text{-}b)\ \sigma_E\ d\zeta/dt$ (Box III).
- Combining the previous equations yields the **initial value problem** $d\zeta/dt\ (a\text{-}b)\ \sigma_E = K\ (v - v_p)$.
- Periodically, we impose an earthquake by applying a **step change in velocity** (i.e. stress state) (Box IV)
- To ensure independence of initial conditions, we **spin up** the earthquake cycle **until stationary behavior**.
- Using **Green's functions**, we calculate **surface displacement timeseries $\mathbf{d^{pred}(t)}$** (Box VI).

VI. Surface Observations & Example Forward Model Results

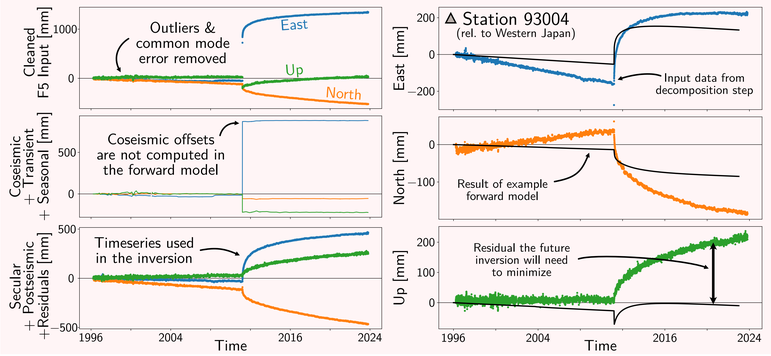

- We use the **F5** surface observations provided by **GEONET** (Takamatsu et al., 2023).
- Using **DISSTANS** (Köhne et al., 2023), we **remove effects not included in our forward model** (coseismic steps, maintenance steps, seasonal oscillations, volcanic transients and slow slip events) to yield $\mathbf{d^{obs}(t)}$.
- We **reference the timeseries** (both observed and modeled) to the average motion of 10 stations in Western Japan.

References

1. Agata, R., Barbot, S. D., Fujita, K., Hyodo, M., Iinuma, T., Nakata, R., et al. (2019). Rapid mantle flow with power-law creep explains deformation after the 2011 Tohoku mega-quake. Nature Communications, 10(1), 1385.
2. Blanpied, M. L., Lockner, D. A., & Byerlee, J. D. (1995). Frictional slip of granite at hydrothermal conditions. Journal of Geophysical Research: Solid Earth, 100(B7), 13045–13064.
3. Bürgmann, R., & Dresen, G. (2008). Rheology of the Lower Crust and Upper Mantle: Evidence from Rock Mechanics, Geodesy, and Field Observations. Annual Review of Earth and Planetary Sciences, 36(1), 531–567.
4. Freed, A. M., Hashima, A., Becker, T. W., Okaya, D. A., Sato, H., & Hatanaka, Y. (2017). Resolving depth-dependent subduction zone viscosity and afterslip from postseismic displacements following the 2011 Tohoku-oki, Japan earthquake. Earth and Planetary Science Letters, 459, 279–290.
5. Fukuda, J., & Johnson, K. M. (2021). Bayesian Inversion for a Stress-Driven Model of Afterslip and Viscoelastic Relaxation: Method and Application to Postseismic Deformation Following the 2011 MW 9.0 Tohoku-Oki Earthquake. Journal of Geophysical Research: Solid Earth, 126(5).
6. Hayes, G. P., Moore, G. L., Portner, D. E., Hearne, M., Flamme, H., Furtney, M., & Smoczyk, G. M. (2018). Slab2, a comprehensive subduction zone geometry model. Science, 362(6410), 58–61.
7. Hetland, E. A., & Simons, M. (2010). Post-seismic and interseismic fault creep II: transient creep and interseismic stress shadows on megathrusts. Geophysical Journal International, 181(1), 99–112.
8. Hetland, E. A., Simons, M., & Dunham, E. M. (2010). Post-seismic and interseismic fault creep I: model description. Geophysical Journal International, 181(1), 81–98.
9. Hirth, G. (2002). Laboratory Constraints on the Rheology of the Upper Mantle. Reviews in Mineralogy and Geochemistry, 51(1), 97–120.
10. Hirth, G., & Kohlstedt, D. (2004). Rheology of the Upper Mantle and the Mantle Wedge: A View from the Experimentalists. In Inside the Subduction Factory (pp. 83–105). American Geophysical Union (AGU).
11. Kanda, R. V. S., Hetland, E. A., & Simons, M. (2013). An asperity model for fault creep and interseismic deformation in northeastern Japan. Geophysical Journal International, 192(1), 38–57.
12. Köhne, T., Riel, B., & Simons, M. (2023). Decomposition and Inference of Sources through Spatiotemporal Analysis of Network Signals: The DISSTANS Python package. Computers & Geosciences, 170, 105247.
13. Minson, S. E., Simons, M., & Beck, J. L. (2013). Bayesian inversion for finite fault earthquake source models I—theory and algorithm. Geophysical Journal International, 194(3), 1701–1726.
14. Muto, J., Moore, J. D. P., Barbot, S., Iinuma, T., Ohta, Y., & Iwamori, H. (2019). Coupled afterslip and transient mantle flow after the 2011 Tohoku earthquake. Science Advances, 5(9), eaaw1164.
15. Rice, J. R., & Ruina, A. L. (1983). Stability of Steady Frictional Slipping. Journal of Applied Mechanics, 50(2), 343–349.
16. Takamatsu, N., Muramatsu, H., Abe, S., Hatanaka, Y., Furuya, T., Kakiage, Y., et al. (2023). New GEONET analysis strategy at GSI: daily coordinates of over 1300 GNSS CORS in Japan throughout the last quarter century. Earth, Planets and Space, 75(1), 49.

VII. Inverse Model & Simplified Synthetic Test Results

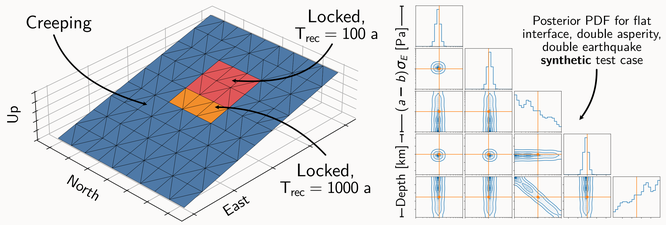

- **Markov-Chain Monte-Carlo (MCMC) framework:** maximize the likelihood $p(\mathbf{d^{obs}}|\theta) = N(\mathbf{d^{obs}}|g(\theta), C_X)$, matching the entire timeseries (not a functional fit), yielding the **posterior distribution $\mathbf{p(\theta|d)}$** for parameters $\theta = \{(a\text{-}b)\ \sigma_E, \text{depths}\}$ using the CATMIP algorithm (Minson et al., 2013) as implemented in the AlTar software.
- **Errors:** observations $\mathbf{d^{obs}} = g(\theta) + \epsilon + e = \mathbf{d^{pred}} + \epsilon + e$, corrupted by observation errors e (covariance C_d currently assumed as constant, diagonal matrix) as well as the model errors ϵ (covariance C_p, currently ignored) with $C_X = C_d + C_p$.
- **Successfully tested** on 2D **synthetic** subduction zones (Köhne et al., *submitted*) and for a flat interface in 3D using synthetic data (left).

VIII. Current Status & Future Work

- We have **successfully recovered** depth-dependent rheological parameters using synthetic data and a **simplified, flat 3D subduction interface with two asperities** (Box VII).
- We have ran the **forward model of the entire earthquake history** in Northern Japan using a **coarse** mesh and non-optimized rheological properties (Box VI).
- The **length of the real earthquake record** (full cycle length approx. 4000 years with more than 400 earthquakes) and mesh size **require computational improvements** to perform timely **inversions**.
- We further aim to improve the **size, shape, and location of the imposed asperities** using published coseismic rupture distributions, and allow the **frictional strength** to vary both down-dip and **along-strike**.